J|A|C|S
ARTICLES

Published on Web 01/15/2009

Conformations of N-Heterocyclic Carbene Ligands in Ruthenium Complexes Relevant to Olefin Metathesis

Ian C. Stewart, Diego Benitez, Daniel J. O'Leary,† Ekaterina Tkatchouk, Michael W. Day, William A. Goddard III, and Robert H. Grubbs*

The Arnold and Mabel Beckman Laboratory of Chemical Synthesis and the Materials and Process Simulation Center, Division of Chemistry and Chemical Engineering, California Institute of Technology, Pasadena, California 91125, and Department of Chemistry, Pomona College, Claremont, California 91711

Received October 6, 2008; E-mail: rhg@caltech.edu

Abstract: The structure of ruthenium-based olefin metathesis catalyst **3** and model π-complex **5** in solution and in the solid state are reported. The *N*-tolyl ligands, due to their lower symmetry than the traditional *N*-mesityl substituents, complicate this analysis, but ultimately provide explanation for the enhanced reactivity of **3** relative to standard catalyst **2**. The tilt of the *N*-tolyl ring provides additional space near the ruthenium center, which is consistent with the enhanced reactivity of **3** toward sterically demanding substrates. Due to this tilt, the more sterically accessible face bears the two methyl substituents of the *N*-aryl rings. These experimental studies are supported by computational studies of these complexes by DFT. The experimental data provides a means to validate the accuracy of the B3LYP and M06 functionals. B3LYP provides geometries that match X-ray crystal structural data more closely, though it leads to slightly less (~0.5 kcal mol^{-1}) accuracy than M06 most likely because it underestimates attractive noncovalent interactions.

I. Introduction

Olefin metathesis has become an indispensible tool for the construction of carbon−carbon bonds and the development of catalysts for this reaction continues to drive development in this burgeoning field.[1] In particular, ruthenium-based catalysts (Figure 1) offer excellent levels of reactivity and selectivity, and their environmental robustness makes them simple to use. Ruthenium catalysts containing a N-heterocyclic carbene (NHC) ligand (e.g., **2**)[2]exhibit high levels of reactivity in a number of reactions that were challenging or impossible for diphosphine catalyst **1**.[3] However, *N*-mesityl catalyst **2** exhibits low efficiency in the formation of sterically encumbered olefins by ring-closing metathesis (RCM) and cross metathesis (CM). These limitations can be circumvented, while preserving the robustness of this catalyst framework, by reducing the steric bulk of the NHC ligand.[4] In particular, *N*-tolyl catalyst **3** has proved rather successful in this regard.[5]

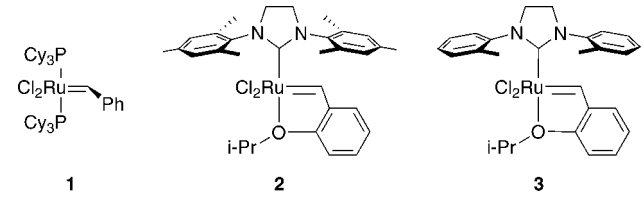

1 **2** **3**

Figure 1

In order to establish a basis for further catalyst development efforts, we investigated the source of this enhanced reactivity. In particular, we expected that the conformation of the *N*-aryl rings of **3** is likely to play a key role. We report here a detailed experimental study using solid- and solution-state investigations of **3** and a model π-bound olefin complex (**5**), as well as a quantum mechanical study using density functional theory (DFT).

The experimental data included in this study provide an excellent basis for validating the accuracy of density functional theory (DFT). DFT calculations with the popular B3LYP functional have become a valuable predictive tool. B3LYP has been shown to provide excellent accuracy on stable intermediates and transition states in main group and transition metal reaction mechanisms.[6] However, there is increasing evidence that B3LYP errs significantly for attractive medium-range

† Current address: Department of Chemistry, Bowdoin College, Brunswick, ME 04011.

(1) (a) Chauvin, Y. *Angew. Chem., Int. Ed.* **2006**, *45*, 3740–3747. (b) Schrock, R. R. *Angew. Chem., Int. Ed.* **2006**, *45*, 3748–3759. (c) Grubbs, R. H. *Angew. Chem., Int. Ed.* **2006**, *45*, 3760–3765. (d) Nicolaou, K. C.; Bulger, P. G.; Sarlah, D. *Angew. Chem., Int. Ed.* **2005**, *44*, 4490–4527. (e) Grubbs, R. H. *Tetrahedron* **2004**, *60*, 7117–7140. (f) *Handbook of Metathesis*, Grubbs, R. H., Ed.; Wiley-VCH: Weinheim, 2003. (g) Schrock, R. R.; Hoveyda, A. H. *Angew. Chem., Int. Ed.* **2003**, *42*, 4592–4633. (h) Frenzel, U.; Nuyken, O. *J. Polym. Sci. Part A: Polym. Chem.* **2002**, *40*, 2895–2916. (i) Trnka, T. M.; Grubbs, R. H. *Acc. Chem. Res.* **2001**, *34*, 18–29. (j) Fürstner, A. *Angew. Chem., Int. Ed.* **2000**, *39*, 3012–3043. (k) Buchmeiser, M. R. *Chem. Rev.* **2000**, *100*, 1565–1604.

(2) Scholl, M.; Ding, S.; Lee, C. W.; Grubbs, R. H. *Org. Lett.* **1999**, *1*, 953–956.

(3) Schwab, P.; France, M. B.; Ziller, J. W.; Grubbs, R. H. *Angew. Chem., Int. Ed.* **1995**, *34*, 2039–2041.

(4) Berlin, J. M.; Campbell, K.; Ritter, T.; Funk, T. W.; Chlenov, A.; Grubbs, R. H. *Org. Lett.* **2007**, *9*, 1339–1342.

(5) (a) Stewart, I. C.; Douglas, C. J.; Grubbs, R. H. *Org. Lett.* **2008**, *10*, 441–444. (b) Stewart, I. C.; Ung, T.; Pletnev, A. A.; Berlin, J. M.; Grubbs, R. H.; Schrodi, Y. *Org. Lett.* **2007**, *9*, 1589–1592. (c) White, D. E.; Stewart, I. C.; Grubbs, R. H.; Stoltz, B. M. *J. Am. Chem. Soc.* **2008**, *130*, 810–811. (d) Enquist, J. A.; Stoltz, B. M. *Nature* **2008**, *453*, 1228–1231. (e) Clark, D. A.; Basile, B. S.; Karnofel, W. S.; Diver, S. T. *Org. Lett.* **2008**, *10*, 4927–4929.

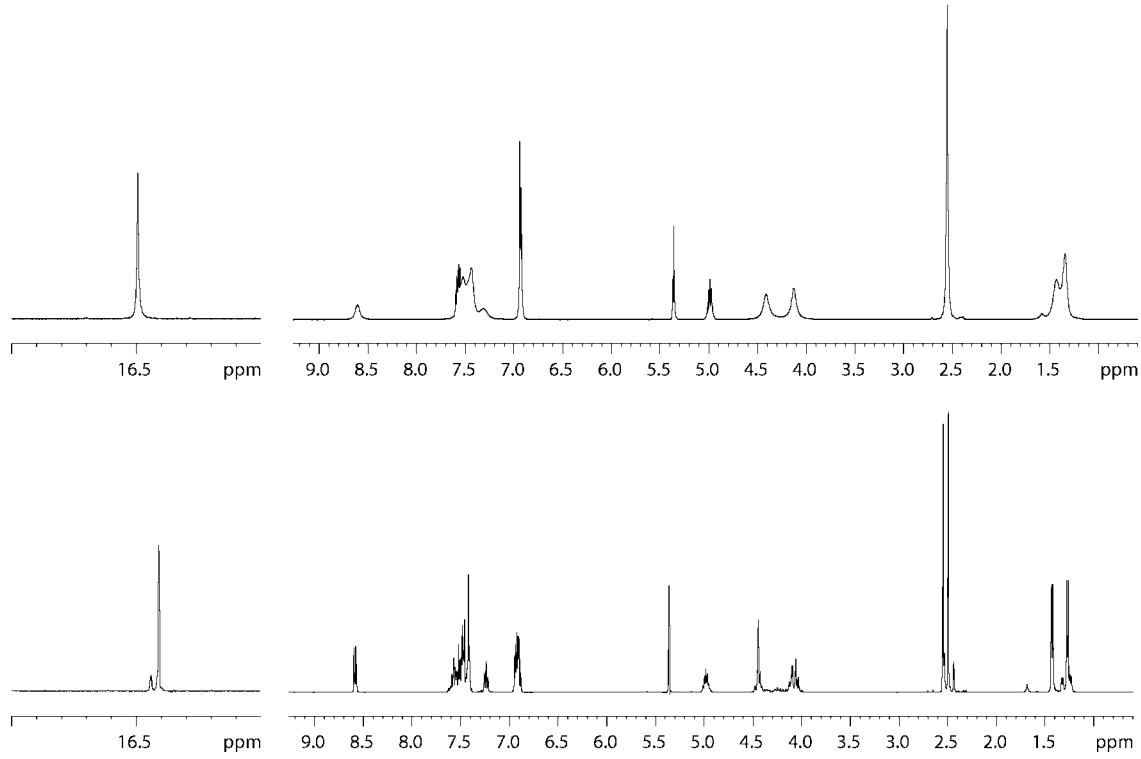

Figure 2. ^{1}H spectra (400 MHz) of complex **3** dissolved in CD_2Cl_2. Top: spectrum recorded at 19 °C. Bottom: spectrum recorded at −48 °C.

attractive interactions such as van der Waals and π-π stacking.[7] Recently, Truhlar reported the M06-class of DFT functionals that were developed with the objective of improving the accuracy in describing medium range attractive interactions.[8]

It was previously shown[9] that B3LYP predicts accurately the energy of intermediates in the isomerization of *cis* and *trans* dichloro Ru complexes relevant to olefin metathesis. In contrast, Truhlar and Zhao reported[8] that medium-range noncovalent interactions (dispersion forces) can have a dramatic effect on the ruthenium tricyclohexylphosphine (PCy_3) bond dissociation energies for Ru-based olefin metathesis catalysts. Given this apparent discrepancy in the accuracy of B3LYP and M06, the accuracy of predicting the relative stability of conformers of *cis* and *trans* dichloro Ru complexes relevant to olefin metathesis with the new M06 functional is assessed herein.[10]

II. Solution-State Structure of Isopropoxybenzylidene 3 via NMR Analysis

The room-temperature ^{1}H NMR spectrum of catalyst **3** (Figure 2, top) shows evidence of an exchange process that produces a single resonance for the benzylidene proton (16.45 ppm) and a single shift for Me_6 and $Me_{6'}$. Most of the aromatic resonances are broadened and one resonance appears distinctively downfield at 8.57 ppm. The NHC backbone resonances split into two broad resonances at 4.37 and 4.09 ppm. The isopropyl methine resonance is sharp, while the isopropyl methyl resonances display separate broad and overlapping peaks.

Upon cooling to −48 °C, the ^{1}H spectrum sharpens, and resonances corresponding to a major and minor form (6.7:1) can be identified (Figure 2, bottom). The benzylidene resonances (H_{Bn}) of the major and minor forms appear at 16.37 and 16.40 ppm, respectively (see Figure 3 for naming scheme). The low-field aromatic resonance sharpens into a one-proton doublet (J = 7.5 Hz). The NHC backbone resonances sharpen into a complex multiplet pattern consistent with four unique chemical shifts. For the major isomer, two resonances are observed for the Me_6 and $Me_{6'}$; a similar spectrum is observed for the minor form. Finally, the isopropyl methyl groups appear as a set of sharp doublets for the major and minor forms.

A 2D-NOESY spectrum recorded at −48 °C revealed that exchange processes were still operative at this temperature and served to interconvert resonances within a given isomer and among the major and minor forms. Analysis of the data provided an estimate of the magnetization transfer rate (k_{for}) between major and minor forms to be 3.9 s^{-1}.

A combination of NMR experiments was used to assign the syn/anti relationship of Me_6 and $Me_{6'}$ in the major conformation (**3a**)

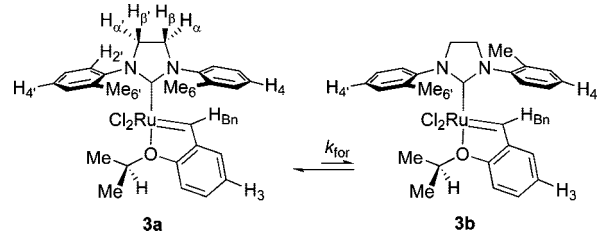

Figure 3

(6) (a) Baker, J.; Muir, M.; Andzelm, J.; Scheiner, A. In *Chemical Applications of Density-Functional Theory*; Laird, B. B., Ross, R. B., Ziegler, T., Eds.; ACS Symposium Series 629; American Chemical Society: Washington, DC, 1996. (b) Niu, S.; Hall, B. M. *Chem. Rev.* **2000**, *100*, 353–405. (c) Nielsen, R. J.; Keith, J. M.; Stoltz, B. M.; Goddard, W. A., III. *J. Am. Chem. Soc.* **2004**, *126*, 7967–7974. (d) Nielsen, R. J.; Goddard, W. A., III. *J. Am. Chem. Soc.* **2006**, *128*, 9651–9660.

(7) Benitez, D.; Tkatchouk, E.; Yoon, I.; Stoddart, J. F.; Goddard, W. A., III. *J. Am. Chem. Soc.* **2008**, *130*, 14928–14929.

(8) Zhao, Y.; Truhlar, D. G. *Org. Lett.* **2007**, *9*, 1967–1970. (b) Zhao, Y.; Truhlar, D. G. *Acc. Chem. Res.* **2008**, *41*, 157–167.

(9) Benitez, D.; Goddard, W. A., III. *J. Am. Chem. Soc.* **2005**, *127*, 12218–12219.

observed in solution at low temperature. From the 2D-NOESY experiment,[11] it was apparent that Me_6 and $Me_{6'}$ both showed through-space interactions with the low-field NHC resonances. The identity and spatial orientation of these two low-field NHC resonances is essential for making the syn/anti $Me_6/Me_{6'}$ assignment. First, a 2D-HMQC experiment established that these two resonances arose from protons attached to different carbon atoms (Figure 4). Second, 1D homonuclear decoupling experiments

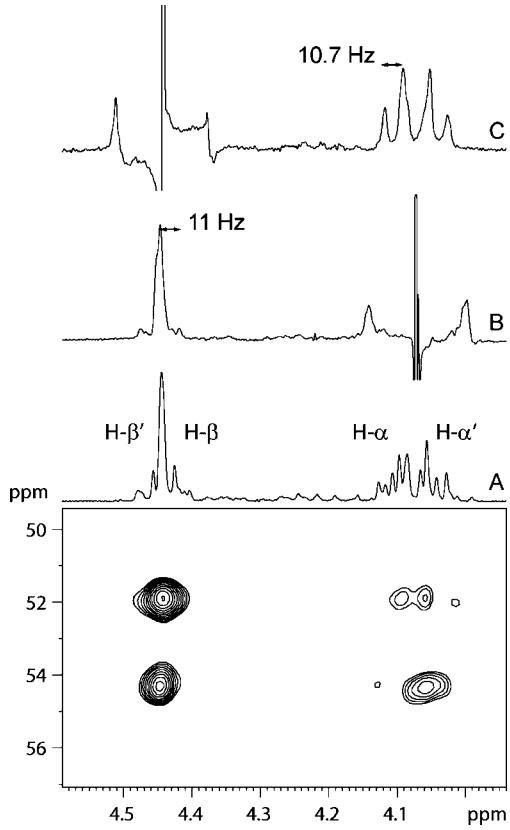

Figure 4. (A) NHC region of 400 MHz ^{1}H 2D-HMQC experiment recorded at −48 °C. The two-proton low- and high-field NHC ^{1}H resonances each correlate to different carbon atoms. (B) 1D spectrum of NHC region with homonuclear decoupling applied at high-field resonance. Low-field resonances collapse to a highly degenerate AB pattern with $J_{AB} = 11$ Hz. (C) NHC region with homonuclear decoupling applied at low-field resonances. High-field resonances collapse to an AB pattern with $J_{AB} = 10.7$ Hz.

established a syn orientation of H_β and $H_{\beta'}$ on the basis of large $H_\beta/H_{\beta'}$ and $H_\alpha/H_{\alpha'}$ vicinal coupling constants (11 and 10.7 Hz, respectively). Analysis of models and a modified Karplus equation suggested that if the vicinal proton pairs in question were each trans, then the couplings would have been in the range of 2−8 Hz. Because Me_6 and $Me_{6'}$ in the major isomer each show an Overhauser effect to a syn pair of NHC backbone protons (H_β and $H_{\beta'}$), their own relationship must likewise be syn.

Further analysis of Overhauser effects provided specific shift assignments. For example, the downfield $Me_6/Me_{6'}$ resonance in **3a** was assigned to Me_6 on the basis of an Overhauser effect between it and H_{Bn}. Another set of conformation-defining Overhauser effects involves the downfield aromatic doublet at 8.54 ppm. This resonance is assigned as $H_{2'}$ on the basis of interactions with the isopropyl methyl resonances, the upfield $Me_{6'}$ resonance, and the upfield resonance of the high field set of NHC resonances ($H_{\alpha'}$).

The minor isomer in solution was assigned to be the conformation with an anti relationship between Me_6 and $Me_{6'}$ because it is the only other reasonable structure to consider. We were unable to obtain definitive proof of this assignment because of limitations in signal-to-noise and peak overlap issues, which were especially problematic in the NHC region.

To summarize this section, compound **3** was found to exist as a mixture of two conformations that interconvert rapidly in solution. The major conformation was found to be the syn conformation in which Me_6 and $Me_{6'}$ are on the same side of the NHC ligand. The minor isomer was assumed to be the other reasonable conformation, in which the two methyl groups are disposed in an anti relationship.

III. Solid-State Structure of Complex 3 via X-Ray Diffraction

Crystals suitable for X-ray diffraction studies were obtained as dark green blocks by vapor diffusion of pentane into a benzene solution of **3**.[12] The NHC ligand is disordered between syn conformation (**3a**) and anti conformation (**3b**) with respect to the *N*-tolyl substituents, with the syn isomer being the major component with ∼91% occupancy (Figure 5). More specifically, the N2-tolyl ring is disordered between these two locations, while the N1-tolyl group is well refined in a single position. Excluding this disorder, the two conformations exhibit similar metric parameters to each other and to *N*-mesityl catalyst **2**. However, the N1-tolyl substituent is rotated ∼35° away from being perpendicular with the NHC plane (as measured by relevant dihedral angles), while the N2-tolyl ring is within 5° of perpendicularity.

IV. Solution State Structure of π-Complex 5 via NMR Analysis

Although the above solution- and solid-state conformational analysis of precatalyst **3** show that both the syn and anti conformations of the *N*-tolyl NHC ligand are accessible, additional models of olefin metathesis intermediates were sought to explain its enhanced reactivity. A number of stable olefin

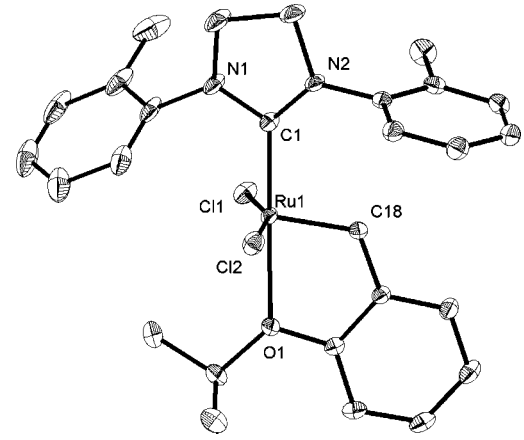

Figure 5. ORTEP diagram of complex **3a**. Selected bond lengths (Å) and angles (deg.): Ru1−C1, 1.9611(11); Ru1−C18, 1.8329(11); Ru1−Cl1, 2.3445(3); Ru1−Cl2, 2.3532(3); Ru1−O1, 2.2979(8); C18−Ru1−C1, 100.45(5); C18−Ru1−O1, 78.71(4); C1−Ru1−O1, 179.15(4); Cl1−Ru1−Cl2, 160.382(12). Thermal ellipsoids are shown at 50% probability.

(10) Truhlar and Zhao performed single point calculations with the M06-L functional on B3LYP optimized structures. Their report suggested that the M06 functional might be much more accurate than B3LYP. Consequently, we performed calculations with the M06 functional on B3LYP and M06-L optimized structures.

(11) See Supporting Information.

π-complexes of ruthenium complexes relevant to olefin metathesis have been reported in recent years.[13] Conveniently, CM of 1,2-divinylbenzene with pyridine-adduct **4** afforded the desired complex (**5**) in good yield (eq 1).

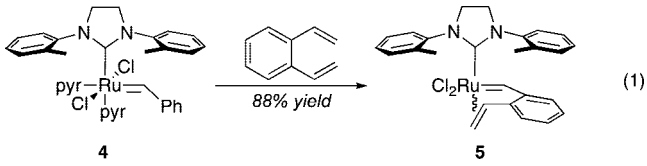

4 **5** (1)

The room temperature ^{1}H NMR spectrum of complex **5** shows four low-field benzylidene resonances with relative integration intensities of 1:10:4:2 (16.24, 16.08, 15.77, and 15.71 ppm, respectively).[11] The remainder of the spectrum is characterized by a mixture of sharp and broad peaks. 2D NOESY/EXSY experiments (600 ms mixing time) conducted at room temperature revealed no exchange occurring among the benzylidene resonances, nor any among the olefin resonances. This contrasts with complex **6**, where exchange was observed to occur among the two principal olefin complexes in solution (a 2:3 mixture of **6a** and **6b** was observed).[13a] It should be noted that exchange is also not observed in certain other Ru−olefin complexes.[13d] Another difference in behavior of complexes **5** and **6** is that Ru−C_{NHC} bond rotation is observable only in the latter. Therefore, it appears that the conformers adopted by **5** at room temperature are less labile than those of complex **6**. Additionally, there is qualitative evidence for the enhanced chemical stability of complex **5** relative to complex **6**: when dissolved in dichloromethane and stored in a sealed NMR tube held at −20 °C, complex **5** appeared to be stable for months, whereas solutions of complex **6** typically would show signs of decomposition within a week.

On a 400 MHz (^{1}H) spectrometer, it was necessary to cool the sample to −82 °C in order to sharpen the spectral lines sufficiently to probe the geometry of the major complexes. Although a fast exchange process between major conformer **5a** and a fifth and minor conformer was likely active at room temperature, cooling to −82 °C allowed a fifth minor benzylidene resonance to be observed. The chemical shifts of all benzylidene resonances were also found to be temperature-dependent. H_{Bn} resonances were observed in a 1:15:165:64:27 ratio (16.06, 16.01, 15.86, 15.4, and 15.32 ppm, respectively).

At −82 °C the major conformer exhibited the following NMR parameters for the bound olefin resonances: H_a, 4.89 ppm (dd, J = 12.0, 9.0 Hz); H_b, 2.05 ppm (d, J = 9.0 Hz); and H_c, 2.83 ppm (d, J = 12.0 Hz). The chemical shifts of the geminally disposed H_a and H_b resonances (see Figure 6 for naming scheme) are shifted even further upfield than in complexes **6a/6b**, where these resonances ranged from 3.4 to 3.7 ppm. At −82 °C, a 2D-NOESY experiment revealed Overhauser interactions between H_a and the two ortho methyl resonances ($Me_{6'}$ and Me_6) at 2.55 and 1.42 ppm. An NOE was also observed between H_{Bn} and the H_2 resonance at 7.91 ppm. These interactions are consistent with a side-bound olefin geometry in which the olefinic CH_2 group is oriented away from syn-disposed Me_6 and $Me_{6'}$ (**5a**). A 2D-COSYLR experiment, which can detect very small scalar couplings (<1 Hz) between protons, revealed a coupling between H_{Bn} and H_b at 2.05 ppm. Formally operating through six bonds, this type of coupling has been observed in other side-bound Ru−olefin complexes.[13] The precise mechanism of this coupling remains unknown, but participation of the metal center may play a role.

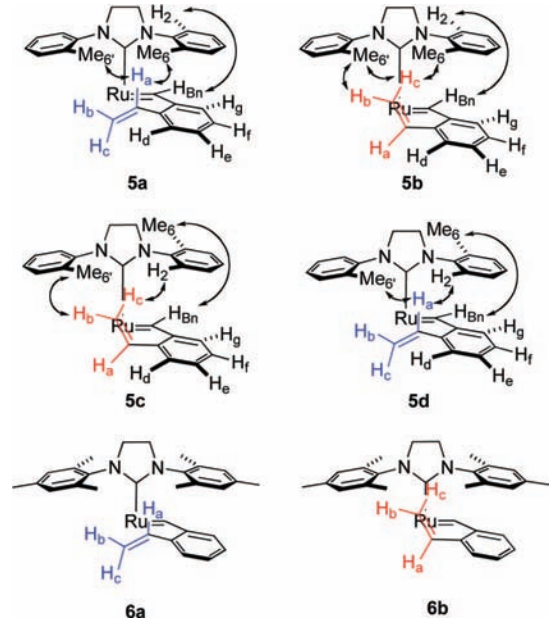

Figure 6. Naming scheme for ^{1}H NMR resonances in complexes **5** and **6**. Selected observed NOEs are indicated with double-headed arrows. Color has been used to clarify the geometry of the bound olefin (blue, side-bound, CH_2 down; red, side-bound, CH_2 up). Chloride ligands are omitted for clarity.

The bound olefin resonances for the second-most populated conformer (H_{Bn} 15.40 ppm) exhibited NMR parameters of H_a, 5.71 ppm (dd, J = 11.8, 10.0 Hz); H_b, 2.98 ppm (d, J = 10.0 Hz); H_c, 2.92 ppm (dd, J = 11.8 Hz). At −82 °C, Overhauser interactions were observed between H_c and two methyl resonances at 2.39 and 1.17 ppm. NOEs were also observed between H_b and the methyl resonance at 2.39 ppm and between H_{Bn} and the H_2 resonance at 8.1 ppm. These Overhauser effects would be expected to arise in a side-bound olefin geometry in which the olefinic CH_2 group is oriented toward syn-disposed ortho methyl groups Me_6 and $Me_{6'}$ (**5b**). A long-range H_{Bn}/H_b coupling was also observed in this complex.

While the structural assignment of complexes **5a** and **5b** could be based upon the observation of several Overhauser effects, the remaining three complexes were more difficult to characterize with Overhauser effects because of low signal-to-noise ratios and peak overlap issues. Despite this difficulty, it is possible to use chemical shift arguments coupled with key NOE observations to provide evidence for the geometry of two of the remaining complexes.

In the third-most populated conformer (H_{Bn} 15.32 ppm) and in complexes **5a** and **5b**, an NOE between H_{Bn} and H_g at 6.75 ppm is clearly evident. This NOE is to be expected, as the benzylidene proton is always proximal to the ortho-disposed H_g. In the cases of complexes **5a** and **5b**, however, there was additional and structure-determining NOE between H_{Bn} and one downfield aromatic resonance, assigned as H_2. On the other hand, for structure **5c**, H_{Bn} does not have a discernible NOE to any other aromatic resonances but it does have an NOE between H_{Bn} and a methyl

(12) Crystallographic data have been deposited at the CCDC, 12 Union Road, Cambridge CB2 1EZ, UK and copies can be obtained on request, free of charge, by quoting the publication citation and the deposition number 635259.

(13) (a) Anderson, D. R.; Hickstein, D. D.; O'Leary, D. J.; Grubbs, R. H. *J. Am. Chem. Soc.* **2006**, *128*, 8386–8387. (b) van der Eide, E. F.; Romero, P. E.; Piers, W. E. *J. Am. Chem. Soc.* **2008**, *130*, 4485–4491. (c) Tallarico, J. A.; Bonitatebus, P. J.; Snapper, M. L. *J. Am. Chem. Soc.* **1997**, *119*, 7157–7158. (d) Anderson, D. R.; O'Leary, D. J.; Grubbs, R. H. *Chem. Eur. J.* **2008**, *14*, 7536–7544.

resonance at 2.92 ppm. Therefore, this signal was assigned as Me_6. Whereas Me_6 in complexes **5a** and **5b** was oriented proximal to the bound olefin, in **5c** it appears to occupy the alternate position and lies over the benzylidene proton. An additional argument can be made in support of this orientation in complex **5c** and **5d**. In earlier studies of complex **6** and as discussed above for complexes **5a** and **5b**,[13a] methyl groups occupying the quadrant shown by Me_6 in **5a** and **5b** tended to be shielded relative to other NHC-derived methyl resonances. There are only two shielded Me resonances in the spectrum of the mixture, and these have been assigned to **5a** and **5b**. All other methyl resonances are not shielded, which suggests that the methyl groups have changed their orientation in the two remaining complexes. This was confirmed for complex **5c** by the observation of an NOE between a reasonably shielded H_2 (6.0 ppm) and H_c of the olefin. The identity of the shielded doublet as H_2 was confirmed by establishing scalar and NOE connectivity between it and H_3 (6.713 ppm), H_4 (7.38 ppm), H_5 (7.52 ppm), and Me_6 (2.905 ppm). This shielding effect for the aromatic H_2 is likely to have an origin similar to that described earlier for Me_6 in complexes **5a** and **5b** providing a useful means for establishing structure. The olefin resonances were partially characterized with parameters: H_a, 5.76 ppm (dd, $J = 10$, 12 Hz); H_b, 2.83 ppm (d, $J = 10$ Hz); and H_c, 2.59 ppm (d, $J = 12$ Hz). The shifts for H_a and H_b are similar to those observed for the same nuclei in **5b**, and a long-range coupling is observed between H_b and H_{Bn}. These similarities suggest a side-bound olefin with the CH_2 group oriented toward the NHC ligand. Additional evidence is required to define the orientation of $Me_{6'}$. As was the case in complexes **5a** and **5b**, NOEs involving the olefin resonances and portions of the NHC ligand are useful for making this assignment. The H_a resonance, which is reasonably well isolated at 5.76 ppm, was not observed to have any interesting NOEs beyond that to the cis-disposed H_b resonance at 2.83 ppm. This would be expected for the olefin binding geometry as shown in **5c**. An NOE was observed between H_b and a methyl resonance at 2.37 ppm, which is consistent with $Me_{6'}$ being proximal to the bound olefin.

The three olefin resonances in the fourth-most populated conformer (H_{Bn} 16.01 ppm) were assigned as H_c, 3.03 ppm (d, $J = 12$ Hz); H_b, 2.03 ppm (d, $J = 10$ Hz); H_a, (5.10 ppm, dd, $J = 10$, 12 Hz). An NOE between H_a and a strongly shielded aromatic doublet at 5.61 ppm provided evidence for a side-bound complex in which the olefinic CH_2 group is oriented away from the NHC ligand. The identity of the shielded doublet was confirmed as arising from H_2 by establishing scalar and NOE connectivity between it and H_3 (6.22 ppm), H_4 (7.08 ppm), H_5 (7.235 ppm), and Me_6 (2.546 ppm). An NOE was observed between H_{Bn} and Me_6, which confirms the orientation of these two groups as shown in structure **5d**. Again a strong degree of correspondence was observed between the olefinic chemical shifts in **5d** and the structurally similar complex **5a**. The orientation of the 'left' NHC-derived aromatic residue in complex **5d** likely has $Me_{6'}$ facing the olefin, although this assignment is based upon the observation of an NOE between H_a and a methyl resonance that overlaps with Me_6 at 2.546 ppm. No NOEs were observed between H_a and any other aromatic chemical shifts, which lends further support for the proposed geometry.

Summarizing this section, a variety of NMR experiments were employed to assign the structure of the four conformations of π-complex **5** observed at −82 °C. The structure of the fifth and most minor (ca. 0.4% of the sample) conformation, **5e**, could not be established because of low signal-to-noise NOE data. The two major conformations, **5a** and **5b**, accounting for ~84% of the sample, display syn-disposed methyl groups that are oriented toward the π-coordinated olefin ligand. These results are counterintuitive given the increased reactivity of catalyst **3** (i.e., we expected the methyl groups to be oriented away from the coordinated olefin, which would explain the tolerance of **3** for sterically demanding substrates). To obtain the structural information needed to resolve this issue, we expanded our analysis of **5** to the solid state.

V. Solid State Structure of π-Complex 5 via X-Ray Diffraction

Crystals suitable for X-ray diffraction studies were obtained as olive green blocks by vapor diffusion of benzene into a dichloromethane solution of **5**.[14] As with complex **3**, the conformational disorder for the *N*-tolyl substituents was observed in the solid state, and further complications arise because the space group ($Pca2_1$) can be problematic.[15] There are two molecules in the asymmetric unit related by an apparent center of symmetry. A number of atoms are not related through this apparent center, which gives us a high degree of confidence in our assignment. Although evidence of the disorder is apparent for both molecules, it could only be modeled in one of the pair. This disorder corresponds to two of the five conformations observed in the solution state. The first, constituting 68% occupancy, is complex **5b** in which the methyl groups are displayed in a syn orientation and the bound olefin is oriented up toward them (Figure 7, top). The remainder of this molecule is conformation **5d** wherein the methyl groups are in an anti conformation and the olefin points downward, away from the NHC (Figure 7, bottom).

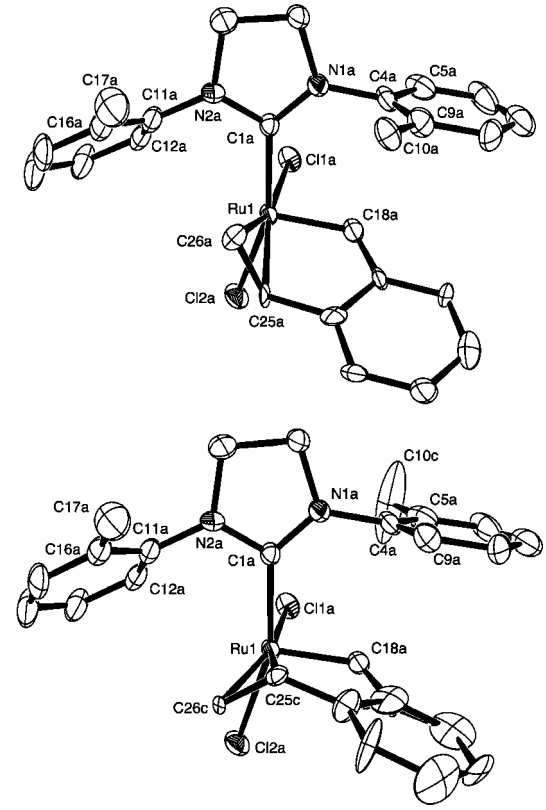

Figure 7. ORTEP diagrams of complexes **5b** (top) and **5d** (bottom). Thermal ellipsoids are shown at 50% probability.

Even though **5a**, the most stable conformation in solution, was not detected in the solid state, the X-ray structural data does provide an important clue as to the source of the reactivity

difference between the *N*-tolyl complex **5** and the *N*-mesityl analogue **6**. Significant rotation (30°) around the N2a−C11a bond was observed by measuring appropriate dihedral angles in the structures of **5b** and **5d** (and **6a** for comparison, see Table 1). This twisting of the N1-tolyl ring provides additional space for the coordinated olefin, and methylene carbon C26a in particular.

Table 1. Comparison of Relevant Dihedral Angles Showing *N*-Aryl Twisting in **5d** and **6a**

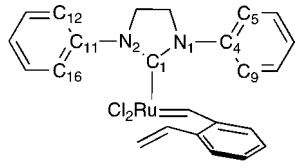

	5d	6a
$C_1-N_2-C_{11}-C_{16}$	121.70	83.89
$C_1-N_2-C_{11}-C_{12}$	−59.36	−100.86
$C_1-N_1-C_4-C_9$	94.67	91.01
$C_1-N_1-C_4-C_5$	−88.41	−94.59

Summarizing this section, X-ray diffraction analysis revealed structural details of two of the five conformations of complex **5** in the solid state. In these structures the 'left' *N*-tolyl ring is tilted significantly away from the bound olefin, in contrast to complex **6**, for which the *N*-mesityl rings are within 10° of bisecting the NHC plane. This tilting of the *N*-aryl rings is likely due to the absence of a substituent on the face opposite to the bound olefin, as **5d** and **6a** present otherwise nearly identical steric environments to the bound olefin. However, without structural evidence for the major conformation in solution (**5a**), we turned our attention to quantum mechanical calculations.

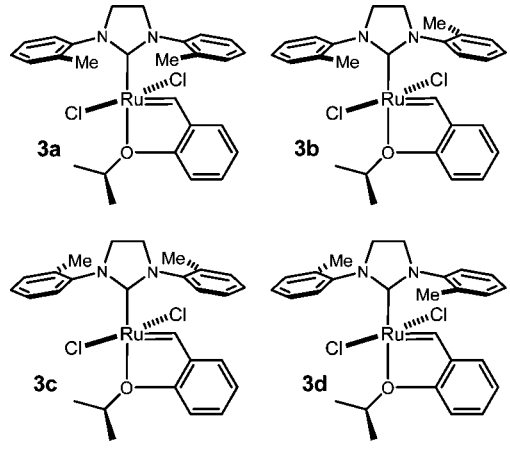

Figure 8. Isomers of **3** calculated with the B3LYP and M06 functionals.

VI. Quantum Mechanical Calculations[16]

Isopropoxybenzylidene Catalyst (3). For catalyst **3**, two relevant rotations that generate two sets of different syn and anti isomers were indentified. The rotation about the NHC-aryls generates **3a** and **3b**, while the rotation about the NHC−Ru bond leads to two new syn and anti isomers (**3c** and **3d**) where the *i*PrO group points to opposite sides of the catalyst (see Figure 8 for naming scheme).[17] We believe that these structures contribute to the total population of syn and anti isomers, and are therefore relevant in our theoretical analysis.

Table 2 shows that B3LYP and M06 predict (CH_2Cl_2 at 225 K) the syn configuration as most stable in agreement with our ^{1}H NMR interpretation. In the gas phase, M06 predicts that **3a** is more stable than **3b** by 0.56 kcal mol^{-1} (∼75% of **3a**) which is consistent with **3a** the most abundant (91%) isomer present in the solid state. In solution, M06 predicts both syn isomers (**3a** and **3c**) to be the most stable complexes in a combined ratio of 7:1 in excellent agreement with experiment (6.7:1). Our results show that B3LYP is able to make good qualitative predictions, and that M06 exhibits remarkably accurate quantitative predictions in the stability of organometallic complexes.

1,2-Divinylbenzene as Chelating Ligand (5). The 2-methyl substitution of the NHC-aryls leads to 12 possible isomers when coordinated with 1,2-divinylbenzene. All 12 isomers were minimized with B3LYP and with M06-L with the LACVP+** basis set and computed energies with B3LYP and M06 functionals with the LACV3P++**(2f) basis set. Figure 9 shows an overlay graphic comparison of the B3LYP and M06-L optimized structures (full color) over the X-ray structure (orange) of complex **5b**. It is clear that B3LYP predicts a geometry in closer resemblance to experiment. The attractive dispersion forces in M06-L favor the stacking of the *o*-tolyl and the 1,2-divinyl aryls. Overestimation of the stacking tendency causes a distortion in the placement of the coordinated olefin. The olefin coordination distance in the X-ray structure is 2.17 Å compared to 2.17 Å from B3LYP and 2.12 Å from M06-L. However, both methods predict the Ru-NHC distance 0.03 Å too long (2.03 Å X-ray and 2.06 Å B3LYP and M06) while for the benzylidene Ru=C distance, M06-L predicts 1.87 Å, B3LYP predicts 1.85 Å (1.84 Å X-ray). The aryl-NHC dihedral angles in **5b** are relatively well predicted with unsigned mean errors of 4.25° and 2.89° for M06-L and B3LYP, respectively.

The predicted geometry of **5d** shows similar peculiarities in the geometries optimized by B3LYP and M06-L (see Figure 10). B3LYP does a better job at predicting the solid-state geometry, while M06-L overemphasizes the aryl−aryl attractive medium-range interactions that distort the dihedral of the NHC-*o*-tolyl and 1,2-divinylbenzene ligand.[18] In contrast, M06-L accurately predicts the solid-state geometry of complexes **3a** and **3b** (see the Supporting Information) because the aryl ring of the benzylidene ligand lies perpendicular to the aryl rings of the NHC ligand, thus eliminating the susceptibility to $\pi-\pi$ stacking.

Table 2. Comparison for M06 and B3LYP Predicted Relative Free Energies (ΔG_{225}) and Abundances of Isomers of **3** in CH_2Cl_2 at 225 K

geometry	B3LYP	B3LYP	M06-L	B3LYP	B3LYP	M06-L	experiment
SP energy	B3LYP	M06	M06	B3LYP	M06	M06	
structure		relative energy (kcal mol^{-1})[a]			relative abundance		^{1}H NMR
3a	0.13	0.0	0.0	2.9	1.2	7.0	6.7 (syn)
3c	0.0	0.37	0.45				
3b	0.75	0.66	1.15	1	1	1	1 (anti)
3d	0.40	0.04	0.95				

[a] $G_{TOT} = E_{SCF} + E_{SOLV} + E_{ZP} + H_{VIB} - TS_{VIB}$.

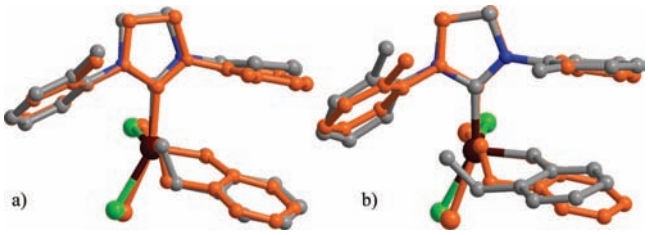

Figure 9. Comparison of the geometries of the (a) B3LYP and (b) M06-L minimized structures of **5b** overlaid with the XRD structure in orange.

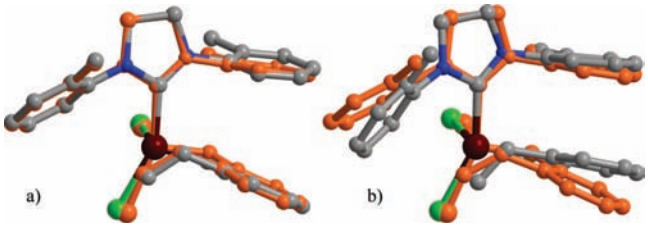

Figure 10. Comparison of the geometries of the (a) B3LYP and (b) M06-L minimized structures of **5d** overlaid with the XRD structure in orange.

The predicted energy differences for the isomers of **5** are presented in Table 3 (see Figure 11 for naming scheme). Complex **5a** is predicted by B3LYP and M06 as the most stable isomer in CH_2Cl_2 at 298 K. The differences arise in the relative energy of the rest of the isomers. M06 predicts that **5a** exists almost exclusively (>95%), while B3LYP predicts the coexistence of five major isomers (>1%) with similar relative abundances as experiment. B3LYP also predicts the coexistence of **5e** which was presumably not observed experimentally. Interestingly, the M06 functional with the B3LYP geometry predicts **5e** as the second most abundant isomer.

VII. Conclusions

Structural aspects of catalyst **3** and π-bound olefin complex **5** were studied by a combination of solution- and solid-state structural analysis, alongside computational studies. We were surprised by the prevalence of conformations in which the two *N*-tolyl rings were displayed in a syn orientation. Furthermore, for π-complex **5** the two most prevalent isomers (**5a** and **5b**) not only exhibit syn-disposed *N*-tolyl rings, but the methyl groups are oriented *toward* the bound olefin. In order to accommodate this congestion, the aryl rings of the NHC are rotated away from the bound olefin, which brings only a small hydrogen substituent closer to the metal center. In other words, the substituted side of the *N*-aryl rings appears "smaller" than the unsubstituted face due to rotation of these rings. This (initially counterintuitive) hypothesis was also proposed by Cavallo in regards to olefin binding to chiral ruthenium-based olefin metathesis catalysts.[19] Thus, we believe that in moving from *N*-mesityl catalyst **2** to *N*-tolyl catalyst **3**, the observed increase in reactivity is due to accessibility of conformations in which the *N*-aryl rings are rotated away from approaching and coordinated olefins.

We show that the B3LYP flavor of DFT predicts geometries for Ru metathesis relevant complexes in better agreement with experiment than M06-L. This suggests to us that the attractive noncovalent interactions are overemphasized in M06-L. B3LYP and M06 both predict relative energies of isomers in very good

Table 3. Comparison for M06 and B3LYP Predicted Relative Free Energies (ΔG_{298}) and Abundances of Isomers of **5** in CH_2Cl_2 at 298 K

geometry	B3LYP	B3LYP	M06-L	B3LYP	B3LYP	M06-L	experiment
SP energy	B3LYP	M06	M06	B3LYP	M06	M06	
structure		relative energy (kcal mol^{-1})[a]			relative abundance		^{1}H NMR
5a	0.0	0.0	0.0	9.8	15.9	95.9	10
5b	0.36	0.44	2.21	5.4	7.6	2.3	4
5c	0.29	0.78	2.82	6.0	4.3	0.8	2
5d	1.35	1.64	2.70	1.0	1.0	1.0	1
5e	0.25	0.02	4.88	6.5	15.4	0.0	N.O.
5f	1.67	1.98	5.61	0.6	0.6	0.0	N.O.
5g	1.70	2.57	7.76	0.6	0.2	0.0	N.O.
5h	2.01	1.95	8.89	0.3	0.6	0.0	N.O.
5i	4.21	6.67	8.17	0.0	0.0	0.0	N.O.
5j	4.10	6.70	8.63	0.0	0.0	0.0	N.O.
5k	2.80	5.61	7.30	0.1	0.0	0.0	N.O.
5l	4.28	7.33	9.62	0.0	0.0	0.0	N.O.

[a] $G_{TOT} = E_{SCF} + E_{SOLV} + E_{ZP} + H_{VIB} - TS_{VIB}$.

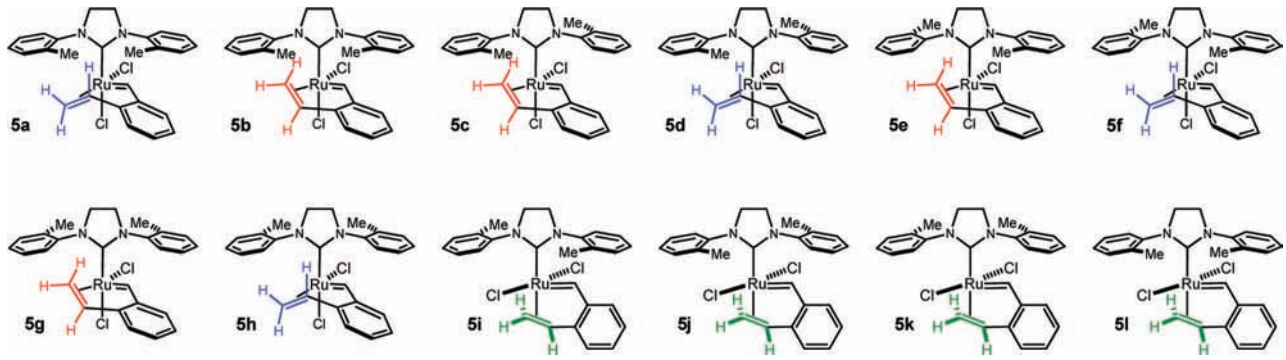

Figure 11. Isomers of **5** calculated with B3LYP and M06 functionals. Color has been used to clarify the geometry of the bound olefin (blue, side-bound, CH_2 down; red, side-bound, CH_2 up; green, bottom-bound).

agreement to ^{1}H NMR experimental observations, with M06 being remarkably accurate, ~0.5 kcal mol mol^{-1} better than B3LYP.

Acknowledgment. The NIH (F32GM078734 and K99GM084302 to I.C.S., 5RO1GM31332 to R.H.G.), the NSF (NIRT(CTS-0608889) to D.B., E.T., W.A.G., CHE-0410425 to R.H.G.) and Pomona College Chemistry Department (to D.J.O.) for generous financial support. Larry Henling for X-ray crystallography assistance. Computational facilities were funded by grants from ARO-DURIP and ONR-DURIP. D.B. and E.T. thank Dr. Vyacheslav Bryantsev for help with NWChem and Professor Donald G. Truhlar for helpful discussions. NWChem Version 5.1, as developed and distributed by Pacific Northwest National Laboratory, P. O. Box 999, Richland, Washington 99352, and funded by the U.S. Department of Energy, was used to obtain some of these results. The Bruker KAPPA APEXII X-ray diffractometer was purchased via an NSF CRIF:MU award to the California Institute of Technology, CHE-0639094.

Supporting Information Available: Details of NMR experiments and computational data; complete ref 18a. This material is available free of charge via the Internet at http://pubs.acs.org.

JA8078913

(14) Crystallographic data have been deposited at the CCDC, 12 Union Road, Cambridge CB2 1EZ, UK and copies can be obtained on request, free of charge, by quoting the publication citation and the deposition number 693207.
(15) Marsh, R. E.; Schomaker, V.; Herbstein, F. H. *Acta Crystallogr.* **1998**, *B54*, 921–924.
(16) Calculations were performed on all systems using density functional theory (DFT) with the B3LYP, M06 and M06-L functionals, as implemented in Jaguar 7.0 (release 207). Jaguar 7.0 Release 207, Schrodinger, LLC, New York, NY, 2006. See Supporting Information for more details on the methods.
(17) This rotation can also be interpreted as a rotation along the $(CH_3)_2HC-$OAr bond.
(18) We performed geometry optimizations of **5b** and **5d** using M06-L and a similar basis set with NWChem 5.1 software package and observed no differences in the equilibrium geometries. For NWChem see: (a) Straatsma, T. P.; et al. *NWChem, A Computational Chemistry Package for Parallel Computers, Version 5.1*; Pacific Northwest National Laboratory, Richland, WA, 2007. See Supporting Information for complete reference. (b) High Performance Computational Chemistry: an Overview of NWChem a Distributed Parallel Application. Kendall, R. A.; Aprà, E.; Bernholdt, D. E.; Bylaska, E. J.; Dupuis, M.; Fann, G. I.; Harrison, R. J.; Ju, J.; Nichols, J. A.; Nieplocha, J.; Straatsma, T. P.; Windus, T. L.; Wong, A. T. *Comput. Phys. Commun.* **2000**, *128*, 260–283.
(19) Costabile, C.; Cavallo, L. *J. Am. Chem. Soc.* **2004**, *126*, 9592–9600.